Formation and Fate of Benzimidazole-Based Quinone Methides. Influence of pH on Quinone Methide Fate

Edward B. Skibo[1]

Department of Chemistry, Arizona State University, Tempe, Arizona 85287-1604

Received March 12, 1992 (Revised Manuscript Received July 20, 1992)

The influence of pH on quinone methide fate was assessed from a comparative hydrolytic study of benzimidazole hydroquinones and their *O*-methylated analogues. Elimination of a leaving group from the hydroquinones affords the carbocation or the quinone methide depending on the pH. The *O*-methylated analogues, on the other hand, can only afford the carbocation species. Evidence is presented herein that the quinone methide species is reversibly protonated to afford the carbocation species. The acid dissociation constant for this equilibrium is pK_a 5.5. Above pH 5.5, the quinone methide species traps both nucleophiles and the proton. Below pH 5.5, the quinone methide species is protonated to afford the carbocation species, which exclusively traps nucleophiles. Therefore, the carbocation acid dissociation constant can be used to predict quinone methide fate as a function of pH.

Many naturally occurring quinones are functionalized with a leaving group so as to permit formation of an alkylating quinone methide species upon quinone reduction and elimination of the leaving group.[2] Reductive alkylating systems of this type often exhibit antitumor activity, perhaps due to the low reduction potential of some solid tumors.[3] Work in this laboratory has, therefore, been directed toward the study of heterocyclic reductive alkylating agents as cancer drugs.[4-10] A particularly fruitful area of endeavor has been the study of benzimidazole-based alkylating agents. One such agent, the pyrrolo-[1,2-*a*]benzimidazole in Chart I, was found to possess DNA cleaving and antitumor properties.[10-12] Another agent is the methoxylated benzimidazole in Chart I which alkylates the reduced FAD cofactor of xanthine oxidase.[13] These examples prompted an indepth study of benzimidazole quinone methide and carbocation chemistry, the results of which are described in this report.

From a comparative hydrolytic study of benzimidazole hydroquinones and their *O*-methylated analogues, it was possible to assess the influence of pH on quinone methide fate. Previous studies of daunomycin[14] and mitomycin C[15] have noted a pH dependency for quinone methide fate. The present study, which was carried over a pH range of 0 to 9, provides evidence of quinone methide protonation (see inset of Chart I). The protonated quinone methide is a carbocation that only traps nucleophiles. On the other hand, the quinone methide traps nucleophiles and electrophiles such that the product ratio is *independent* of pH.

Chart I

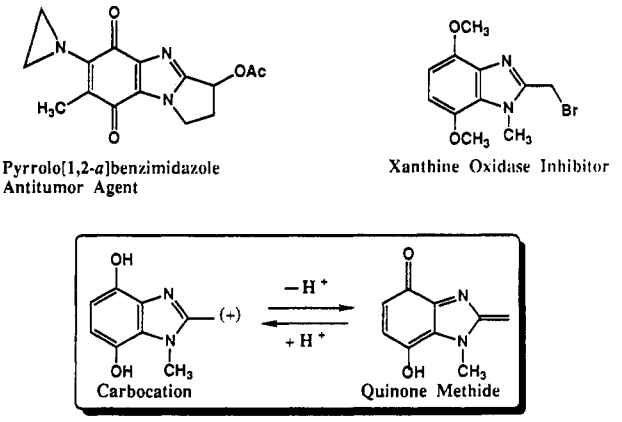

Scheme I

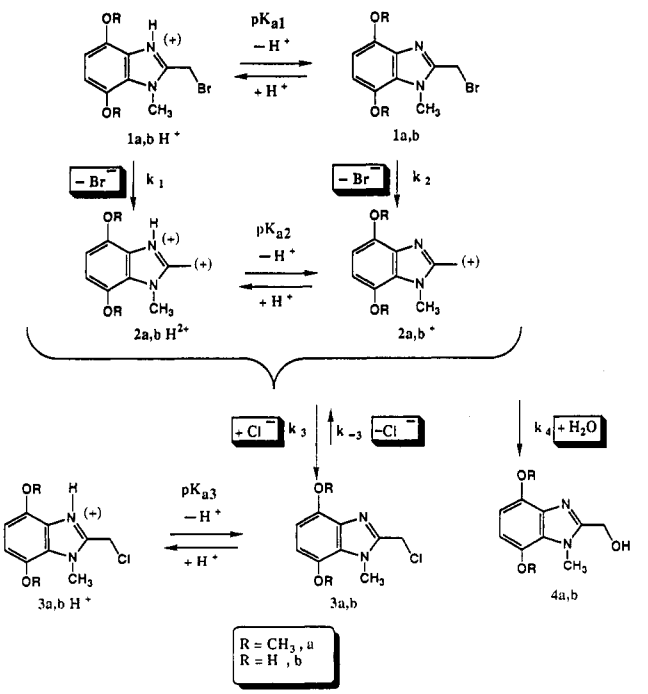

Results and Discussion

Preliminary results of hydrolytic studies of **1a** have appeared in a paper on xanthine oxidase cofactor alkylation.[13] The hydrolysis of **1b** above pH 6 was reported in a paper dealing with quinone methide chemistry.[4]

(1) National Institutes of Health Research Career Development Award Recipient (CA01349), 1988-1993.
(2) (a) Moore, H. W. *Science (Washington, D.C.)* **1977**, *197*, 527. (b) Moore, H. W.; Czerniak, R. *Med. Res. Rev.* **1981**, *1*, 249.
(3) (a) Kennedy, K. A.; Teicher, B. A.; Rockwell, S.; Sartorelli, A. C. *Biochem. Pharm.* **1980**, *29*, 1. (b) Lin, A. J.; Sartorelli, A. C. *Biochem. Pharm.* **1976**, *25*, 206. (c) Kennedy, K. A.; Sligar, S. G.; Polomski, L.; Sartorelli, A. C. *Biochem. Pharmacol.* **1982**, *31*, 2011. (d) Kennedy, K. A.; Rockwell, S.; Sartorelli, A. C. *Cancer Res.* **1980**, *40*, 2356. (e) Keyes, S. R.; Heimbrook, D. C.; Fracasso, P. M.; Rockwell, S.; Sligar, S. G.; Sartorelli, A. C. *Adv. Enz. Reg.* **1985**, *23*, 291.
(4) Skibo, E. B. *J. Org. Chem.* **1986**, *51*, 522.
(5) Lee, C. H.; Gilchrist, J.; Skibo, E. B. *J. Org. Chem.* **1986**, *51*, 4787.
(6) Lee, C.-H.; Skibo, E. B. *Biochemistry* **1987**, *26*, 7355.
(7) Skibo, E. B.; Gilchrist, J. H. *J. Org. Chem.* **1988**, *53*, 4209.
(8) Lemus, R. H.; Skibo, E. B. *J. Org. Chem.* **1988**, *53*, 6099.
(9) Lemus, R. H.; Lee, C.-H.; Skibo, E. B. *J. Org. Chem.* **1989**, *54*, 3611.
(10) Islam, I.; Skibo, E. B. *J. Org. Chem.* **1990**, *55*, 3195.
(11) Islam, I.; Skibo, E. B.; Dorr, R. T.; Albert, D. S. *J. Med. Chem.* **1991**, *34*, 2954.
(12) Skibo, E. B.; Islam, I. U.S. Patent 5015742.
(13) Skibo, E. B. *Biochemistry* **1986**, *25*, 4189.
(14) (a) Gaudiano, G.; Frigerio, M.; Bravo, P.; Koch, T. H. *J. Am. Chem. Soc.* **1990**, *112*, 6704. (b) Gaudiano, G.; Koch, T. H. *Chem. Res. Toxicol.* **1991**, *4*, 2 (see page 9).
(15) (a) Tomasz, M.; Lipman, R. *J. Am. Chem. Soc.* **1979**, *101*, 6063. (b) Tomasz, M.; Lipman, R. *Biochemistry* **1981**, *20*, 5056. (c) Kohn, H.; Zein, N. *J. Am. Chem. Soc.* **1983**, *105*, 4105.

0022-3263/92/1957-5874$03.00/0

Scheme II

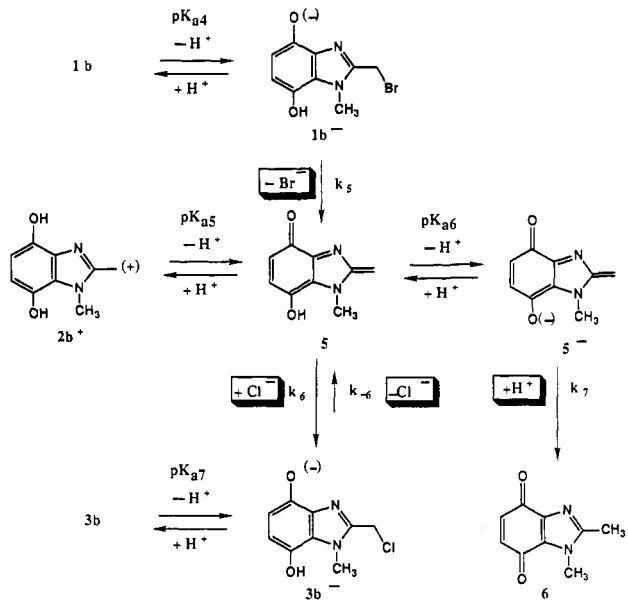

The hydrolysis of benzimidazole hydroquinones **1b** and the *O*-methylated analogues **1a** was studied over the pH range of 0 to 9 in μ = 1.0 (KCl) buffer, see Schemes I and II for structures. Strict anaerobic conditions were employed for hydrolysis studies of air-sensitive hydroquinones. The *O*-methylated derivatives are not air-sensitive, and therefore aerobic conditions can be employed for hydrolysis studies of these analogues. Repetitive scanning results (not shown) revealed that the conversion of bromo derivatives **1a,b** to the chloro derivatives **3a,b** is accompanied by a substantial absorbance change at 240 nm. The conversion of **3a,b** to the hydroxy derivatives **4a,b** is likewise accompanied by a large absorbance change at this wavelength. Thus, it was possible to follow the change of substituents at the 2α-position of the benzimidazole systems during hydrolysis. Above pH 6, quinone methide formation from **1b** and **2b** results in a quinone product, whose formation was followed spectrally at 430 nm. The results of the above hydrolysis studies are outlined below.

***O*-Methylated hydroquinone 1a** hydrolyzed by a two consecutive first-order (biphasic) rate law over the pH range of 0 to 9. The first kinetic phase resulted from the conversion of **1a** to **3a** and the second kinetic phase resulted from the conversion of **3a** to **4a**. Evidence of the intermediacy of **3a** was obtained from isolation, ^{1}H-NMR, and kinetic studies. The preparative hydrolysis of **1a** afforded **3a** when the reaction time extended over 2.7 half-lives of the first kinetic phase. After a long period of time, the final product was **4a**.[13] If chloride is not present in the buffer (pH 5, 1 M acetate), then **4a** and the 2α-acetate are obtained as first kinetic phase products. The hydrolysis reaction was also carried out in pD 6.95 (μ = 1.0, KCl) buffer and the 2α-proton resonances were monitored by repetitive ^{1}H-NMR scans. In this experiment, the resonance for the chloromethyl derivative (**3a**) rapidly built up followed by slow buildup of the hydroxymethyl derivative **4a**. Kinetic evidence of the **3a** intermediate came from the observations that rates for the second kinetic phase of **1a** hydrolysis could be duplicated with authentic **3a**.

Rate data for the first kinetic phase are plotted as the log vs pH in Figure 1. The shape of this pH–rate profile indicates the presence of plateaus for neutral and protonated **1a** (pK_a for acid dissociation from **1aH**$^+$ is 4.09).

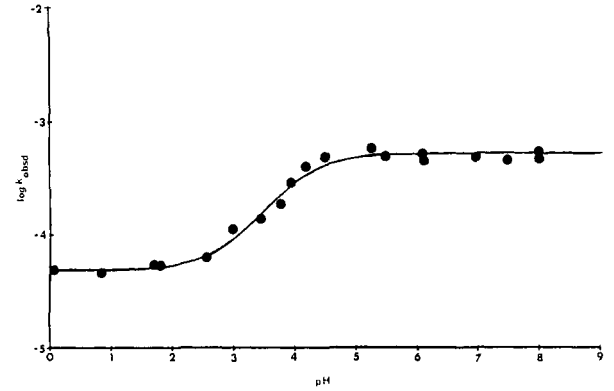

Figure 1. Plot of log k_{obsd} vs pH for the first kinetic phase of **1a** hydrolysis obtained under aerobic conditions.

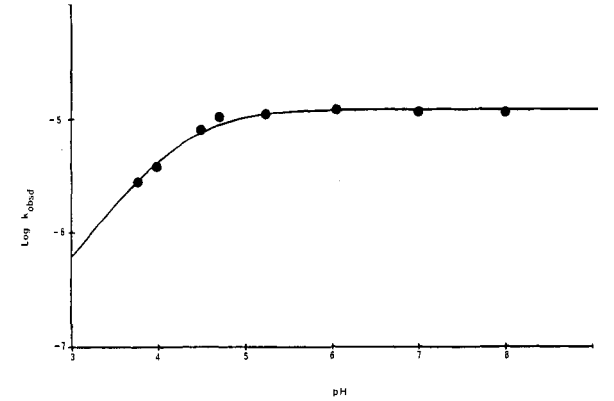

Figure 2. Plot of log k_{obsd} vs pH for the second kinetic phase of **1a** hydrolysis obtained under aerobic conditions.

Accordingly, the mechanism in Scheme I shows bromide elimination from both forms of **1a** to afford the carbocations **2aH**$^{2+}$ and **2a**$^+$. Trapping of these carbocations by chloride in a non-rate-determining step then affords the observed product **3a**.

The pH–rate law for the process described above is derived considering material balance in **1aH**$^+$ and **1a**

$$k_{obsd} = \frac{k_1 a_H + k_2 K_{a1}}{a_H + K_{a1}} \quad (1)$$

where k_1, k_2, and K_{a1} are constants shown in Scheme I and a_H is the proton activity determined with a pH meter. Computer fitting of the data in Figure 1 to eq 1 provided $k_1 = 4.9 \times 10^{-5}$ s^{-1}, $k_2 = 5.2 \times 10^{-4}$ s^{-1}, and $pK_{a1} = 4.01$. This solution was used to generate the solid line shown in Figure 1.

The kinetically obtained value for pK_{a1} closely matches the measured value of 4.09. The near identity of the kinetic and independently measured pK_a values supports the mechanism in Scheme I. A substantial pK_a difference would be an indication of a more complex mechanism.[16] The other mechanisms described below also exhibit near identity in kinetic and independently measured pK_a values.

Rate data for the second kinetic phase are plotted as the log vs pH in Figure 2. The shape of this profile indicates that only the neutral form of **3a** reacts to form product. Thus there is only one plateau in the pH region where neutral **3a** is the predominant species (pK_a for **3aH**$^+$ is 4.11). The conversion of **3a** to **4a** is presumed to occur by reversible carbocation formation from **3a** followed by irreversible trapping of the carbocation species. Consider-

(16) Schmir, G. L.; Bruice, T. C. *J. Am. Chem. Soc.* **1959**, *81*, 4522.

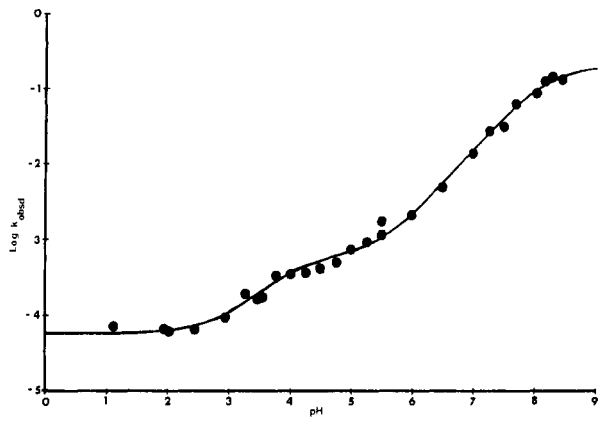

Figure 3. Plot of log k_{obsd} vs pH for the first kinetic phase of **1b** hydrolysis obtained under anaerobic conditions.

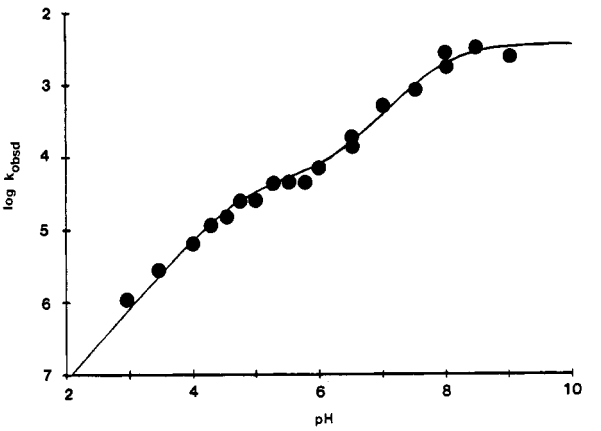

Figure 4. Plot of log k_{obsd} vs pH for the second kinetic phase of **1b** hydrolysis obtained under anaerobic conditions.

ation of this mechanism, material balance in **3a** and **3aH$^+$**, and the presence of steady-state concentrations of **2a** provides the rate law in eq 2

$$k_{obsd} = \frac{\bar{K}k_{-3}K_{a3}}{a_H + K_{a3}} \qquad (2)$$

$$\bar{K} = \frac{k_4 a_{H_2O}}{k_3 a_{Cl} + k_4 a_{H_2O}}$$

where k_{-3}, k_3, K_{a3}, and k_4 are constants in Scheme I, a_H is the proton activity, and a_{Cl} is the chloride activity. Fitting eq 2 to the data in Figure 2 provides $\bar{K}k_{-3} = 1.23 \times 10^{-5}$ and pK_{a3} = 4.28. The kinetically obtained value for proton dissociation from **3aH$^+$** is nearly identical to the measured value of 4.11.

The mechanism shown in Scheme I shows the intermediacy of a carbocation species for both substitution reactions. Thus, added azide did not affect the rate of hydrolysis although the 2α-azide derivative was obtained as the product (see ref 13 for a description of this study). This observation requires that the nucleophilic trapping occur after the rate-determining formation of the carbocation species.

Hydroquinone 1b also hydrolyzed by a two consecutive (biphasic) first-order rate law over the pH range of 1–8.5. The first kinetic phase products are the chloromethyl derivative **3b** in the 1–5.5 pH range and both **6** and **3b** in the 5.5–8.5 pH range. In the second kinetic phase, **3b** is converted to the hydroxymethyl derivative **4b** over the 1–5.5 pH range and to the quinone **6** over the 5.5–8.5 pH range. Reactions occurring in both pH ranges are illustrated in Schemes I and II.

In the present study, the formation of **3b** and **4b** was verified by ^{1}H-NMR studies of the reaction of pD 4.00 buffer (μ = 1.0, KCl) and by kinetic studies. ^{1}H-NMR scans showed the formation of **3b** from **1b** followed by the slow buildup of **4b**. Consistent with the intermediacy of **3b**, the second kinetic phase rates could be duplicated by starting with authentic **3b**. A previous report described the formation of **3b** and **6** during hydrolysis of **1b** in the 6–8 pH range.[4]

Rate data for the first kinetic phase are plotted as the log vs pH in Figure 3. This pH–rate profile shows three plateaus corresponding to involvement of the N(1)-protonated hydroquinone (pK_a = 3.99), the neutral hydroquinone (pK_a for hydroxyl proton dissociation = 8.13), and the hydroquinone hydroxyl anion in the rate-determining steps. The mechanisms in Schemes I and II, therefore, show elimination of bromide from each of the three species. The pH–rate law for this process is shown in eq 3 and was derived considering material balance in **1bH$^+$**, **1b**, and **1b$^-$**

$$k_{obsd} = \frac{k_1 a_H^2 + k_2 a_H K_{a1} + k_2 K_{a1} K_{a4}}{a_H^2 + a_H K_{a1} + K_{a1} K_{a4}} \qquad (3)$$

where k_1, k_2, and K_{a1} are constants in Scheme I and k_5 and K_{a4} are constants in Scheme II. Computer fitting of the data in Figure 3 to eq 3 provided $k_1 = 5.9 \times 10^{-5}$ s^{-1}, $k_2 = 5.3 \times 10^{-4}$ s^{-1}, $k_5 = 0.22$ s^{-1}, pK_{a1} = 3.98, and pK_{a4} = 8.13. Consistent with the postulated mechanism, the kinetically obtained value of pK_{a1} is the same as the measured value (3.99). The value of pK_{a4} was not determined independently.

The pH–rate data obtained for **1b** below pH 5.5 are nearly identical with those obtained for **1a**. Note the values for k_1 (4.9×10^{-5} s^{-1} and 5.9×10^{-5} s^{-1}) and k_2 (5.2×10^{-4} s^{-1} and 5.3×10^{-4} s^{-1}) obtained from the hydrolytic studies of **1a** and **1b**, respectively. The hydroxy group exerts nearly the same resonance electron releasing effect as the methoxy group. Therefore, carbocation formation from **1a** and **1b** should in fact occur with identical rate constants.

Dissociation of the hydroxy proton of **1b** (pK_a = 8.13) results in facile bromide elimination at pH values >5.5. Comparison of elimination rate constants for **1b** ($k_2 = 5.3 \times 10^{-4}$ s^{-1}) and **1b$^-$** ($k_6 = 0.22$ s^{-1}) indicates that a 415-fold increase in the elimination rate constant accompanies hydroxyl anion formation. The elimination products are the quinone methide species **5** and **5$^-$**, which either trap chloride or a proton to afford **3b** and **6**, respectively.[4]

Rate data for the second kinetic phase are plotted as the log vs pH in Figure 4. The two plateaus in this figure indicate that both the neutral and hydroxyl anion forms of **3b** react to form product. The reaction below pH 5.5 is thought to involve reversible carbocation formation followed by water trapping of the carbocation species to afford **4b**. Above pH 5.5, the quinone methide is reversibly formed by chloride elimination from **3b$^-$** and is then trapped by a proton to afford **6**. The pH–rate law for this process was derived by considering both material balance in **3b** and **3b$^-$** and the presence of steady-state concentrations of carbocation and quinone methide

$$k_{obsd} = \frac{a_H k_3 \bar{K} K_{a3} + k_{-6}\bar{\bar{K}} K_{a3} K_{a7}}{a_H^2 + a_H K_{a3} + K_{a3} K_{a7}} \qquad (4)$$

$$\bar{K} = \frac{k_4 a_{H_2O}}{k_3 a_{Cl} + k_4 a_{H_2O}} \qquad \bar{\bar{K}} = \frac{k_7 K_{a6}}{k_6 a_{Cl} + k_7 K_{a6}}$$

where the rate and equilibrium constants are those shown

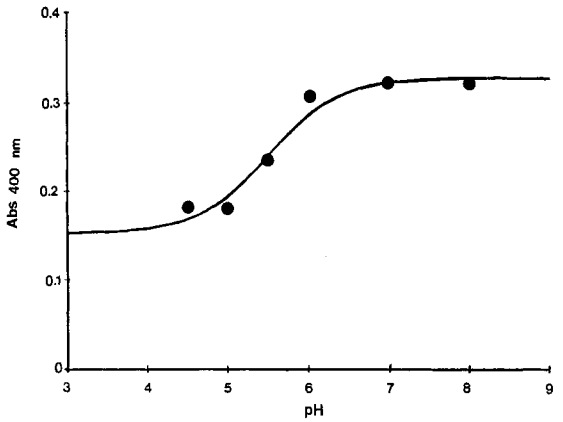

Figure 5. Plot of absorbance (λ = 400 nm) at the conclusion of the first kinetic phase of **1b** hydrolysis vs pH of the reaction mixture. The solid line was computer-generated from eq 6.

in Schemes I and II. Computer fitting the data in Figure 4 to eq 4 provided $\bar{K}k_{-3} = 4.79 \times 10^{-5}$ s^{-1}, $\bar{K}k_{-6} = 3.50 \times 10^{-3}$ s^{-1}, pK_{a3} = 4.76, and pK_{a7} = 7.95. Consistent with the postulated mechanism, the kinetic pK_a values approximate the independently determined values of pK_{a3} and pK_{a7} (4.03 ± 0.18 and 8.4 ± 0.3, respectively).

The rate constant obtained for **3b** hydrolysis below pH 5.5 is in the same range as the rate constant obtained for **3a** hydrolysis. Compare the values for $\bar{K}k_{-3}$ (1.23×10^{-5} s^{-1} and 4.79×10^{-5} s^{-1}) obtained from the hydrolytic studies of **3a** and **3b**, respectively. Both the similar resonance electron releasing properties of the hydroxyl and methoxy groups, and the same carbocation mechanism, account the similarity in rate constants.

Carbocation Acid Dissociation Constant. From the foregoing results, it is apparent that hydroquinones **1b** and **3b** hydrolyze via a carbocation mechanism below pH 5.5. Thus the rate constants and products of hydroquinone hydrolysis are similar to those obtained with the *O*-methylated derivatives **1a** and **3a**, which are known to hydrolyze via a carbocation. Above pH 5.5, hydroquinone hydrolysis proceeds via a quinone methide. The switch from a carbocation to a quinone methide intermediate is proposed to be a consequence of the acid dissociation $\mathbf{2b}^+ \rightleftarrows \mathbf{5} + H^+$.

An estimation of the carbocation acid dissociation constant can be obtained from a plot of quinone **6** concentration vs pH. According to the mechanism in Scheme II, the quinone arises only from the quinone methide species and not from the carbocation. Therefore, the amount of quinone product should be a reflection of the amount of quinone methide formed in the course of hydrolysis. Shown in Figure 5 is a plot of the absorbance of **6** at λ_{max} = 400 nm vs pH. These data were obtained from hydrolysis reactions of **1b** at the conclusion of the first kinetic phase. Fitting the data in Figure 5 to the spectrophotometric pK_a equation (see Experimental Section) provided pK_a = 5.5 ± 0.3, for proton dissociation from carbocation $\mathbf{2b}^+$. This solution was used to generate the solid curve in Figure 5. The absorbance at 400 nm in Figure 5 for pH values <5 is due to trailing from strong absorbance in the UV region. Product studies have in fact verified that **6** is not formed at pH values <5.

If protonation of **5** to afford $\mathbf{2b}^+$ occurred only in strong acid, the ratio of [**3b**]/[**6**] at the conclusion of the first kinetic phase of **1b** hydrolysis would be constant throughout the entire pH range studied. This conclusion is based on the observations that the ratio of [**3b**]/[**6**] is independent of pH above pH 5.5, see ref 4. The mechanism in Scheme II explains why this is so. Formation of **6** involves carbon protonation of the anionic quinone methide ($\mathbf{5}^-$). The proton activity therefore cancels from the rate expression for the formation of **3b** and **6**. The trapping of chloride to afford **3b** also involves the neutral quinone methide species. Since both processes involve the "neutral" quinone methide species regardless of pH, the product ratio is independent of pH. The results shown in Figure 5 show the constant value of [**6**] obtained at pH values >5.5. However, at pH values <5.5, **6** was not isolated nor was it seen spectrally (UV and ^{1}H-NMR). Therefore, it was necessary to invoke the presence of a carbocation intermediate below this pH value.

The protonation of a carbonyl oxygen usually requires very strong acid (pH <0), even when the resulting carbocation is resonance-stabilized.[17] In contrast, the quinone methide **5** is protonated in relatively high pH buffers. The driving force for protonation is probably the conversion of the quinonoid species **5** to the aromatic benzimidazole ring system of $\mathbf{2b}^+$. Indeed the protonation of heptalene to afford an aromatic carbocation is reported to occur with a pK_a > 7.[18]

Conclusions

Evidence is presented that the transient quinone methide species **5** is reversibly protonated to afford carbocation $\mathbf{2b}^+$, pK_a = 5.5 ± 0.3. It is concluded from these studies that other quinone methides, particularly the electron-rich mitomycin and anthracycline species, can be protonated to afford a carbocation species. Another conclusion of this study concerns the influence of quinone methide protonation on quinone methide fate. The generalizations below may pertain to other quinone methides as well as the benzimidazole system **5**. Protonation of the quinone methide results in a carbocation which exclusively traps nucleophiles. The quinone methide itself traps both nucleophiles and protons such that the ratio of trapping products is independent of pH. Therefore, quinone methide fate should vary from nucleophile trapping at low pH values to both proton and nucleophile trapping above the carbocation pK_a. A noteworthy observation is the selective trapping of chloride by the carbocations $\mathbf{2a,b}^+$. Likewise, McClelland and co-workers[19] have observed that the triphenyl carbocation more rapidly combines with chloride than with water. The selective trapping of chloride by $\mathbf{2a,b}^+$ may be due to carbocation stabilization by the electron-releasing hydroxy or methoxy groups resulting in enhanced nucleophile selectivity.[20]

The above conclusions must be applied to the results of other studies with caution. The study described herein was carried out with constant concentrations of chloride nucleophile in aqueous buffers throughout the pH range studied. In contrast, other studies have been carried out with sulfur anionic nucleophiles, the concentrations of which change with pH due to nucleophile protonation. Another contrast is the use of methanolic buffers to slow proton trapping of the quinone methide (see ref 14b and references therein). As a result, the constant ratio of nucleophile and proton trapping with pH may not be observed in these studies. In spite of the above caveats, the results of studies by Tomasz and Lipman, in the area of mitomycin C quinone methide trapping at low pH, are

(17) Steward, R.; Yates, K. *J. Am. Chem. Soc.* **1958**, *80*, 6355.
(18) Dauben, H. J., Jr.; Bertelli, D. J. *J. Am. Chem. Soc.* **1961**, *83*, 4657.
(19) McClelland, R. A.; Banait, N.; Steenken, S. *J. Am. Chem. Soc.* **1986**, *108*, 7023.
(20) (a) Leffler, J. E.; Grunwald, E. *Rates and Equilibria of Organic Reactions*; Wiley: New York, 1963. (b) Giese, B. *Angew. Chem. Int. Ed.* **1977**, *16*, 125. (c) Pross, A. *Adv. Phys. Org. Chem.* **1977**, *14*, 69. (d) McLennan, D. J. *Tetrahedron* **1978**, *34*, 2331.

consistent with the conclusions of the present study. They have observed predominant nucleophile (phosphate) trapping by the mitomycin C quinone methide (carbocation?) at low pH.[15a]

Experimental Section

Hydroquinones and their *O*-methylated derivatives were prepared according to the literature.[4,13] The kinetic studies were carried out in buffers prepared with doubly distilled water and adjusted to $\mu = 1.0$ with KCl. The following buffer systems were employed to hold pH: HCl/water, formic acid/formate (pK_a = 3.6), acetic acid/acetate (pK_a = 4.55), phosphate monobasic/phosphate dibasic (pK_a = 6.50), and boric acid/borate (pK_a = 9.2). These pK_a values were obtained at 30.0 ± 0.2 °C in $\mu = 1.0$ (KCl) aqueous solutions. Measurements of pH were made with a Radiometer GK2401C combination electrode.

Kinetic Studies of Hydrolysis. The hydrolytic studies of the hydroquinones were carried out in anaerobic aqueous buffers employing Thunberg cuvettes as previously described.[21] The *O*-methylated derivatives were studied in aerobic buffer.

Both aerobic and anaerobic studies were carried out as follows: A dimethyl sulfoxide stock of the compound to be studied was prepared fresh and 50 μL of this stock was added to 2.95 mL of buffer. The absorbance vs time data were collected on a UV–vis spectrophotometer in thermostated cells held at 30.0 ± 0.2 °C. These data were computer-fit to the two consecutive first-order equation for the general process A → B → C:[22]

$$\text{absorbance} = Xe^{-k_a t} + Ye^{-k_b t} + Z \tag{5}$$

$$X = \epsilon_A[A_0] - \epsilon_C[A_0] + (\epsilon_B[A_0] - \epsilon_C[A_0])[k_a/(k_b - k_a)]$$

$$Y = \epsilon_C[A_0] - \epsilon_B[A_0][k_a/(k_b - k_a)]$$

$$Z = \epsilon_C[A_0]$$

where $\epsilon_A[A_0]$, $\epsilon_B[A_0]$, and $\epsilon_C[A_0]$ are the maximum possible absorbances of A, B, and C in the process A → B → C, $[A_0]$ is the initial concentration of A, and ϵ's are extinction coefficients of A, B, and C. The first kinetic phase is designated by k_a and the second kinetic phase by k_b. The rate constants plotted on the pH–rate profiles (Figure 1–4) were obtained from the computer fits to the above equation, based on the difference between the data points and the computer-generated curve. Standard errors ranged from 4% for Figures 1 and 2 to 7% for Figures 3 and 4. The absorbance values plotted in Figure 5 were also obtained from such computer fits (absorbance at the conclusion of the first kinetic phase is X in the equation).

pK_a determinations for hydroquinones were carried out in anaerobic aqueous buffer employing Thunberg cuvettes. The pK_a determinations for the *O*-methylated analogues were carried out in aerobic buffers. Both aerobic and anaerobic pK_a determinations were made by computer-fitting absorbance vs pH data, obtained in $\mu = 1.0$ (KCl) 30.0 ± 0.2 °C aqueous buffer, to the following equation

$$\text{absorbance} = \frac{A_T a_H \epsilon_{HA} + A_T \epsilon_A K_a}{a_H + K_a} \tag{6}$$

where A_T is the total concentration of acid and conjugate base ([AH] + [A]), ϵ_{AH} is the extinction coefficient of the acid form, ϵ_A is the extinction coefficient of the conjugate base, a_H is the proton activity determined with a glass electrode, and K_a is the acid dissociation constant obtained from the fit.

^{1}H NMR Studies of Hydrolysis. An ^{1}H-NMR study of the hydrolysis of **1a** (0.015 M) was carried out in DMSO-d_6/0.05 M pD 6.95 phosphate buffer $\mu = 1.0$ (KCl) (3:1) with TSP-d_4 as the reference. The conversion of **1a** to **3a** corresponded to the following chemical shift changes: δ 4.80–4.96 (2-CH_2-X) and 4.02–4.04 (N(1)-CH_3). After 4 days, the final spectrum was that of **4a**: δ 4.86 (2-CH_2OH) and 4.07 (N(1)-CH_3).

An ^{1}H-NMR study of the hydrolysis of **1b** (0.05 M) was carried out in pD 4.00 acetate buffer $\mu = 1.0$ (KCl) under strict anaerobic conditions. The conversion of **1b** to **3b** corresponded to a shift from δ 4.80 to 4.95 for 2-CH_2-X. After several days, the final product **4b** was observed.

Acknowledgment. Funding from the National Institutes of Health and the National Science Foundation is gratefully acknowledged.

(21) Skibo, E. B.; Bruice, T. C. *J. Am. Chem. Soc.* **1983**, *105*, 3304.
(22) Alcock, N. W.; Benton, D. J.; Moore, P. *Trans. Faraday Soc.* **1970**, *66*, 2210.

Syntheses and Diels–Alder Cycloaddition Reactions of 4*H*-Furo[3,4-*b*]indoles. A Regiospecific Diels–Alder Synthesis of Ellipticine

Gordon W. Gribble,* Daniel J. Keavy, Deborah A. Davis, Mark G. Saulnier, Benjamin Pelcman, Timothy C. Barden, Mukund P. Sibi, Erik R. Olson, and Joseph J. BelBruno

Department of Chemistry, Dartmouth College, Hanover, New Hampshire 03755

Received June 10, 1992

Seven examples of the novel 4*H*-furo[3,4-*b*]indole ring system (**3–9**)—a stable, synthetic analogue of indole-2,3-quinodimethane—have been synthesized in 6–8 steps from simple indoles in overall yields of 21–28%. These 4*H*-furo[3,4-*b*]indoles undergo Diels–Alder reactions with several dienophiles (dimethyl acetylenedicarboxylate, *N*-phenylmaleimide, benzyne), including ethyl acrylate, which reacts regiospecifically with furoindole **4** to afford a single carbazole ester (**59**). This result, predicted by molecular orbital calculations, was used to design and execute a regiospecific Diels–Alder synthesis of the antitumor alkaloid ellipticine (**63**). Thus, the trimethylsilyl triflate-induced reaction between furoindole **4** and dihydropyridone **68b** is ≥99% regioselective and affords lactam **70b** in 89% yield. Further manipulation gives ellipticine (**63**) with no detectable (<1%) isoellipticine (**64**) in the crude product.

Over the past ten years, indole-2,3-quinodimethanes (**1**) and their stable cyclic analogues (**2**) have been the focus of considerable interest.[1] Although indole-2,3-quinodimethanes were earlier implicated by Bergman[2] and others[3,4] as intermediates in alkaloid synthesis, and by Hofheinz[5] in alkaloid rearrangement, it was the research of

(1) For an excellent review, see: Pindur, U.; Erfanian-Abdoust, H. *Chem. Rev.* **1989**, *89*, 1681.
(2) (a) Bergman, J.; Carlsson, R. *Tetrahedron Lett.* **1977**, 4663. (b) Bergman, J.; Carlsson, R. *Tetrahedron Lett.* **1978**, 4055.
(3) Driver, M.; Matthews, I. T.; Sainsbury, M. *J. Chem. Soc., Perkin Trans. 1* **1979**, 2506.

0022-3263/92/1957-5878$03.00/0